Open Access Full Text Article

ORIGINAL RESEARCH

Transparent Nano Thin-Film Transistors for Medical Sensors, OLED and Display Applications

Yongbin Hu[1],[*]
Li-Qiang Guo[1],[*]
Changhe Huo[2]
Mingzhi Dai [ID][2,3]
Thomas J Webster [ID][4]
Jianning Ding[1]

[1]Institute of Intelligent Flexible Mechatronics, Jiangsu University, Zhenjiang 212013, People's Republic of China; [2]Ningbo Institute of Materials and Technology Engineering, Chinese Academy of Sciences, Zhejiang 315201, People's Republic of China; [3]Center of Materials Science and Optoelectronics Engineering, University of Chinese Academy of Sciences, Beijing 100049, People's Republic of China; [4]Department of Chemical Engineering, Northeastern University, Boston, MA 02806, USA

*These authors contributed equally to this work

Correspondence: Mingzhi Dai
Email daimz@nimte.ac.cn

Thomas J Webster
Email th.webster@neu.edu

Background: Transparent thin-film transistors (TFTs) have received a great deal of attention for medical sensors, OLED and medical display applications. Moreover, ultrathin nanomaterial layers are favored due to their more compact design architectures.
Methods: Here, transparent TFTs are proposed and were investigated under different stress conditions such as temperature and biases.
Results: Key electrical characteristics of the sensors, such as threshold voltage changes, illustrate their linear dependence on temperature with a suitable recovery, suggesting the potential of the devices to serve as medical temperature sensors. The temperature conditions changed in the range of 28°C to 40°C, which is within the standard human temperature testing range. The thickness of the indium-gallium-zinc oxide semiconductor layer was as thin as only 5–6 nm, deposited by mature radio-frequency sputtering which also showed good repeatability. Optimal bending durability caused by mechanical deformation was demonstrated via suitable electrical properties after up to 600 bending cycles, and by testing the flexible device at a different bending radii ranging from 48 mm to 18 mm.
Conclusion: In summary, this study suggests that the present transparent nano TFTs are promising candidates for medical sensors, OLED and displays which require transparency and stability.
Keywords: flexible, transparent, temperature sensor, transistors, electronic skin

Introduction

For decades, amorphous oxide semiconductor (AOS) thin-film transistors (TFTs) have been widely investigated for numerous sensor applications due to their unique properties, such as transparency and flexibility.[1–5] AOS TFTs based on transparent and flexible substrates could be used as sensors[6] for biological research,[7,8] medical treatment[9] or health monitoring.[10] Transparent TFTs could be used in Organic Light-Emitting Diodes (OLEDs) and displays especially as human-friendly wearable devices and portable electronics for developing IoT.[1,2] However, TFT sensors (such as implantable pressure and strain sensors made of biodegradable materials as reported by Bao et al which have suitable cycle stability[11] and a dual organic transistor tactile-perception element (DOT-TPE) as reported by[12] Zang et al with bio-simulation capabilities) and temperature TFTs sensors lack a compact design and consequently universal acceptance.[13–15] Some use TFTs with thermistors connected to a drain-source electrode in series,[16] while others use a thermo-voltage generator or supercapacitor.[2] However, they are both complex and more compact designs are required. Here, a compact design of only TFTs with channel sensing temperature ability is proposed, fabricated, measured and tested.

The properties of the semiconductor–insulator interface have not been fully understood for such applications.[17] Here, a representative AOS material, ie, indium-gallium-zinc oxide (IGZO), was used as the TFT channel due to its optimal properties including fairly good mobility and excellent transparency.[18,19] IGZO can be formed by low temperature radio-frequency (RF) sputtering processing (no higher than 200°C) as thin as on the order of 1 nm. Polyvinyl alcohol (PVA) was used here as the dielectrics layer, which is a biodegradable material suitable for nano-devices and biomedical research.[20] It is flexible and transparent,[20] and can be formed simply by a spin-coating method.

Here, a transparent temperature TFT sensor is proposed with IGZO as the semiconductor channel and PVA as the insulator layer. Transfer curves of the TFTs and, thus, the current and threshold voltage, change gradually under temperature conditions unidirectionally. This suggests that the devices are a strong candidate for medical temperature sensors. Both of the dielectrics layer or the semiconductor layers could be responsible for the TFTs sensors. According to the experimental results and investigation here, the role of the temperature sensitive layer is to be the channel layer, instead of the dielectrics or gate in the TFTs. The temperature condition ranged from 28°C to 40°C, which is within the standard human temperature range needed for medical applications.

Experimental Section
Fabrication of IGZO-Based TFTs

The transparent TFTs fabricated here can be implemented in a bottom-gate top-contact design. The polyethylene terephthalate (PET) film was selected as the transparent substrate and an amorphous oxide ITO layer was used as the bottom gate. The gate dielectric layer was formed by polyvinyl alcohol, PVA. 10 wt% PVA solutions were prepared by dissolving PVA under atmospheric pressure, by magnetic stirring and heating. The PVA layer was formed by a spin-coating method, with spin-coating conditions of 200 rpm for 3 s, then 2000 rpm for 20 s. Subsequently, the film was heated at 90 for 30 min. Afterwards, the IGZO film was deposited on the PVA dielectric layer by radio-frequency (RF) magnetron sputtering. The flow rate and the pressure were 14 sccm and 0.5 Pa, respectively. The IGZO pattern was made by a self-designed mask. The width and length of the IGZO semiconductor channel were defined as 800 μm and 600 μm, respectively, in the

mask. The ITO drain and source electrodes were then deposited on the channel layer. The source electrode and drain electrode were prepared by electron-beam evaporation or prepared by RF magnetron sputtering. The thickness of the ITO depends on the deposition time of around 140 nm. The width and length of the source-drain electrode mask were 1000 μm and 150 μm, respectively.

Results and Discussion

The schematic of the TFT sensor is shown in Figure 1. While a substrate with flexible and transparent properties such as PET was used, the bottom gate ITO was deposited by RF sputtering. Then, the PVA was deposited with a spin-coating method. Afterwards, the IGZO was deposited in the masks using an RF sputtering method. The electrodes, including the source, drain and cover sheet for the channel, were deposited with a design mask. As shown in Figure 1D, the device films are transparent and flexible.

The key characteristics of TFTs, ie, transfer curves of TFTs sensors, are shown in Figure 2 with the drain voltage V_{DS} as 1.5 V, the gate voltage V_{GS} from - 1 V to 3 V, and the scanning speed as 100 mV/s. The switching ratio of the device could be as large as above 1×10^7. The threshold voltage V_{TH} of the TFTs could be obtained by the intercept of line fitting from the $I_{DS}^{1/2}$-V_{GS} curve. The red curve and the black curve are two curves measured in sequence. While the transfer curve is a typical curve for n-type TFTs, it showed that the device has suitable repeatability. The inset shows that the TFT device under the camera is transparent, with an ITO source and drain electrodes together with the cover sheet on the IGZO channel.

Figure 3 shows a scanning electron microscope (SEM) cross section of the device. It shows the IGZO sputtered on the dielectric layers by the RF sputtering method could be as thin as 5–6 nm, with a surface roughness of less than 1 nm. This is the thinnest reported IGZO ever found by RF sputtering with good electrical properties, ie, less than 10 nm and even might be regarded as a 2-dimensional layer. The electrode layer deposited on the IGZO layer was about 141 nm thick.

Figure 4 shows the temperature impact on the TFTs sensor, with decreasing temperature in blue and increasing temperature in red. It shows that the transfer curves shift in the same direction when the temperature shifts in the same direction. When the temperature increases, the transfer curve shifts to the left. When the temperature decreases, the transfer curve shifts to the right. Figure 5 shows the
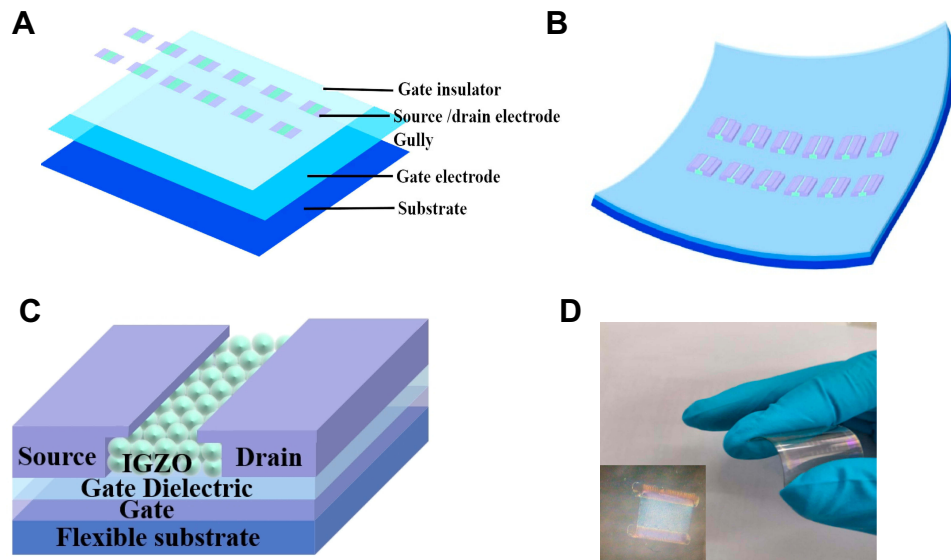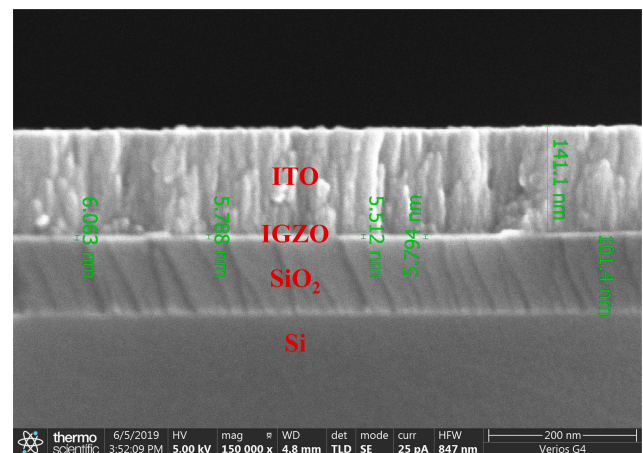
Figure 1 Thin-film transistor-based sensors. (**A, B**) Device structure of TFTs-based on IGZO; (**C**) single TFTs structure; and (**D**) an enlarged image of the flexible transparent temperature medical sensor with a single device.
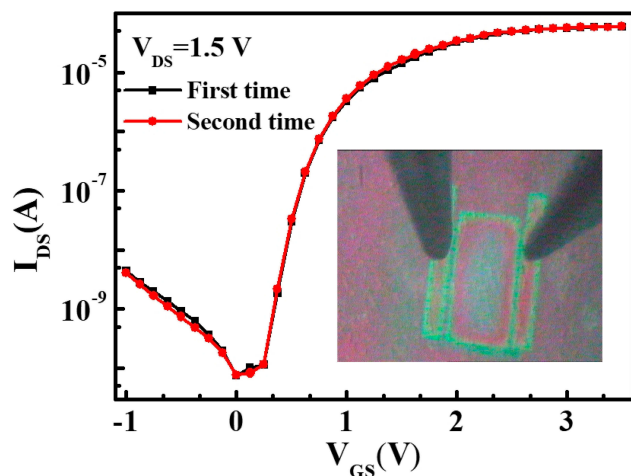
Figure 2 Typical transfer curves of TFTs at room temperature with a good repeatability.


Figure 3 Scanning electron microscopy (SEM) image of TFTs.

transfer curves under different V_{DS} with similar trends of temperature dependence. All of the results suggest that the present TFTs based on IGZO and transparent materials could be used as temperature sensors for numerous medical applications. The negative shift of the transfer curve under higher temperatures is attributed to the hole injections or the oxygen vacancies in AOS which generates additional states near conduction bands and carriers.[21] Channel carriers in AOS could be produced by oxygen vacancies.[21] Heated films could increase the thermally excited oxygen atoms to induce vacancies, which leave the initial positions and enter the interstitial positions.

When the temperature decreases, such oxygen vacancies and interstitial oxygen atoms could recombine.[22,23] Figure 6 supports this mechanism. The stress measurements under a negative gate bias (NBS) and a positive gate bias (PBS) were performed, respectively. When under the bias condition of hole injections (ie, negative gate bias), the negative shift occurs which corresponds to the charge trapping of hole carriers in the interface defect state or the increase of oxygen vacancies.[24–26] This is similar to the phenomena of TFTs sensors under increasing temperatures. When the PBS is performed, the curves shift in a positive way. The trapped electrons generate an additional electric field which could shield the applied electric
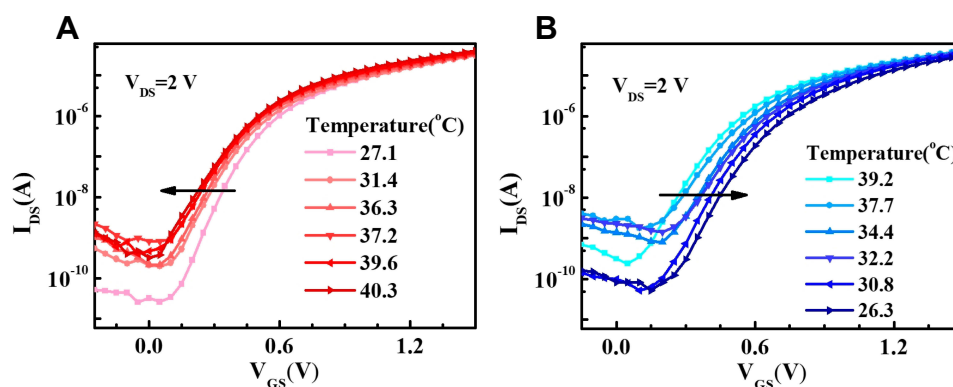
Figure 4 Typical transfer curve degradation of the transparent flexible TFTs samples under temperature stress: Typical transfer curve degradation of transparent flexible TFTs samples during (**A**) heating and (**B**) cooling.
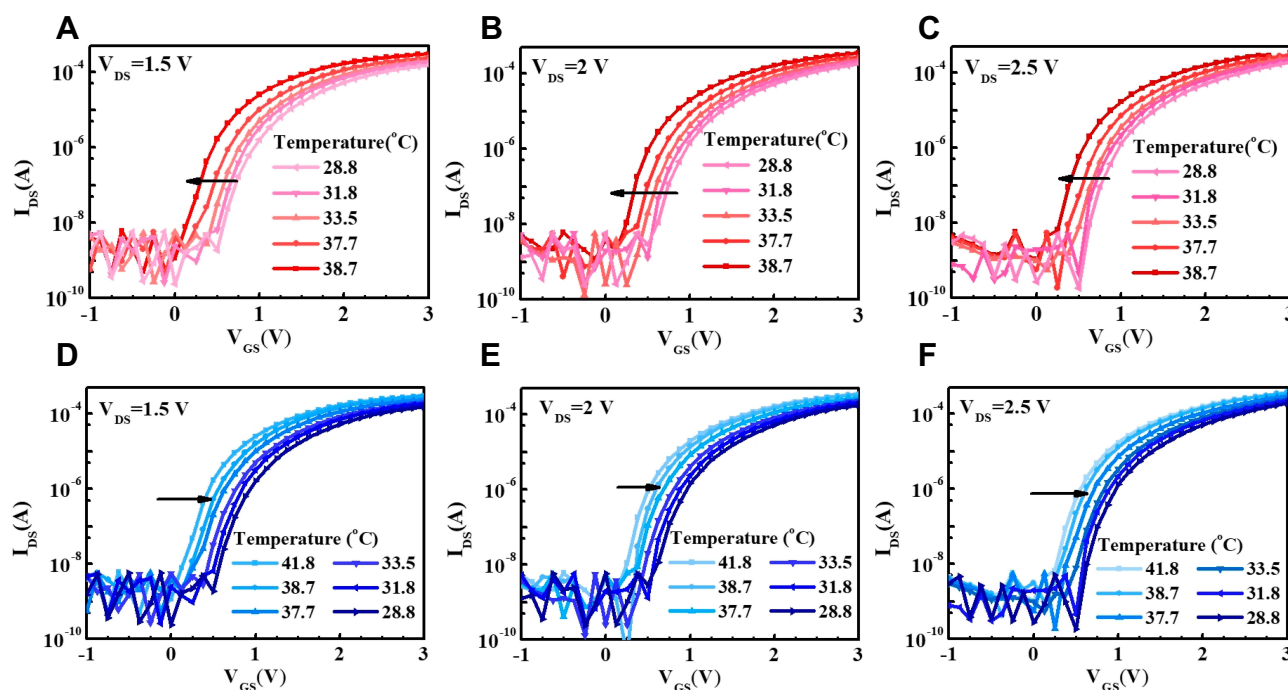
Figure 5 Transfer curve of transparent flexible TFT under source and drain voltages with different temperature stresses.(**A-C**) Under heating conditions,V_{DS} is 1.5 V, 2.0 V and 2.5 V, respectively; (**D-F**) Under cooling conditions, V_{DS} is 1.5 V, 2.0 V and 2.5 V, respectively.

field and require a greater gate voltage to attract the same amount of channel carriers.[27–30] These bias stress experiments could be employed to verify the proposed mechanism of hole/electron injection mechanisms for the TFTs sensors under the temperature conditions used here.

In order to clarify the importance of the dielectric layers and the semiconductor channel layers during the temperature sensing process, the device structure with the dielectrics layer alone (without the a-IGZO semiconductor layer), ie, the capacitor, was fabricated and tested under the temperature conditions. As suggested in Figure 7, the capacitor

was measured under different temperatures ranging from 27°C to 57°C. It shows that while the key electrical properties of the dielectric capacitor change with temperature, the change is relatively small compared to those of the whole TFTs sensors. Therefore, the main change of the electrical properties of the TFTs sensors under temperature stress tests stems from the semiconductor layer.

Figure 8 shows the transmission spectra of the a-IGZO TFTs on the different substrates. Measurements were performed using a UV-visible near-infrared spectrophotometer. The average visible transmittance of the a-IGZO TFTs was
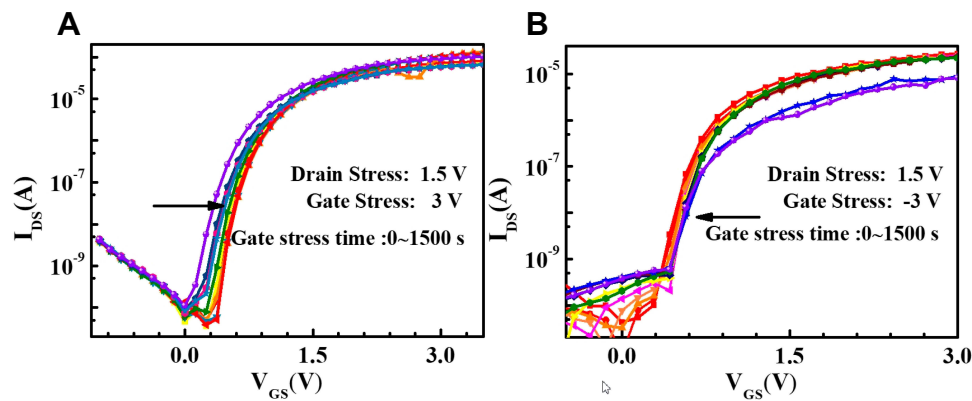
Figure 6 Linear transfer I_{DS}-V_{GS} curve of a-IGZO TFTs as a function of stress time. Evolution of the transfer characteristics of (**A**) device A with increasing positive gate bias time. Evolution of the transfer curves of (**B**) device B with increasing negative gate bias time.
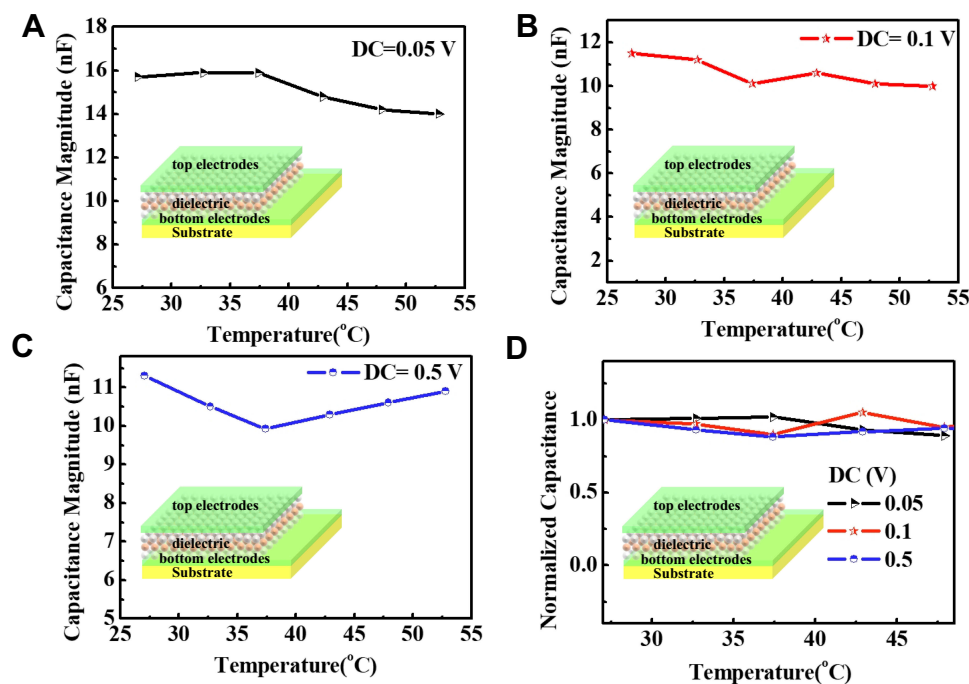
Figure 7 (**A**) The relationship between the gate dielectric capacitance and temperature under a DC voltage of 0.05 V; (**B**) The relationship between the gate dielectric capacitance and temperature under a DC voltage of 0.1 V; (**C**) The relationship between the gate dielectric capacitance and temperature under a DC voltage of 0.5 V; and (**D**) Capacitance of gate dielectric between bottom and top electrodes versus temperature.

larger than 60% in the visible wavelength ranging from 380 to 780 nm.[27–30] The inset of Figure 8B is an optical image of a transparent and flexible a-IGZO TFT on the PET substrate. This result shows that the present devices have good transparency.

Another main concern for wearable electronics is device deformation stability. Figure 9 also shows the flexibility of the TFTs sensor and that the properties stay the same after being bent with angles. The films were bent in the x-axis and y-axis. Results suggest that the TFTs sensors could be used in flexible conditions, with bending,

such as those necessary for portable and wearable electronics. The bending radius of the module is self-designed and made in a 3-dimensional printer with a bending radius of 26.5 mm. In Figure 9, there were no obvious deviations in key electrical properties observed with a bending radius of 26.5 mm in the x or y axes directions.

Conclusion

In general, the TFTs sensor proposed here has optimal temperature sensitivity and transparent properties based on the IGZO semiconductor and PVA dielectric layer. The
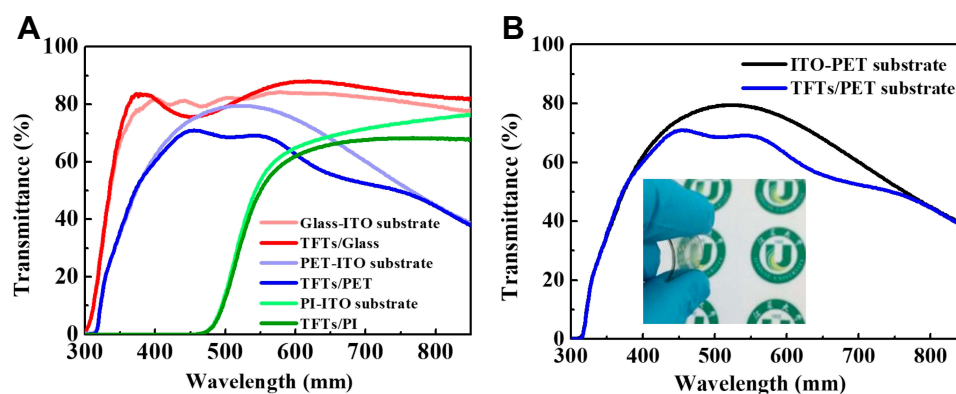
Figure 8 (**A**) Transmission spectra of different substrate materials in the visible range; (**B**) Transmittance spectra of PET substrate and the TFTs/PET in the visible range. Inset in (**B**): The flexible transparent temperature sensor physical image.
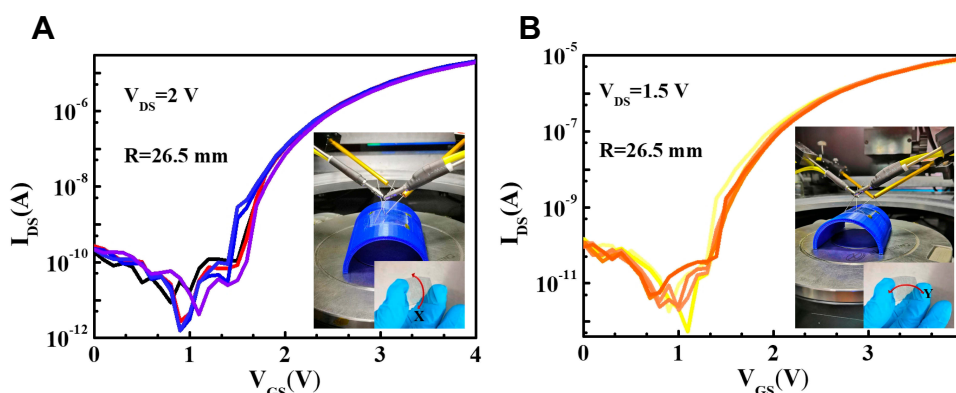
Figure 9 Transfer characteristics of TFT in different bending directions and a bending radius of 26.5mm: (**A**) Transfer curve of TFT under a bending radius of 26.5 mm in the x-direction; (**B**) Transfer curve of TFT under a bending radius of 26.5 mm in the y-direction.

temperature range tested was 28°C to 40°C, perfect for human conditions and numerous medical applications. The transfer curve of the transparent TFTs sensor shifts in the same direction when temperature increases and in the reverse direction when temperature decreases, which may be attributed to hole injections/oxygen vacancy increases and electron injections, respectively. Bias stress measurements were performed to support such mechanisms. The temperature dependence of key sensor properties suggests that such TFTs are a promising candidate for temperature medical sensors. The temperature dependent characteristics mainly come from the IGZO semiconductor layer alone, which suggests that the TFTs sensor could be upgraded by adjusting the semiconductor alone. In summary, this study gives insights into the applications of TFTs sensors for improved transparent and portable electronic devices and nanomedical research.

Acknowledgments

Disclosure

The authors report no conflicts of interest in this work.

References

1. Myny K. The development of flexible integrated circuits based on thin-film transistors. *Nat Electron*. 2018;1(1):30. doi:10.1038/s41928-017-0008-6
2. Lee YH, Jang M, Lee MY, Kweon OY, Oh JH. Flexible field-effect transistor-type sensors based on conjugated molecules. *Chem*. 2017;3 (5):724. doi:10.1016/j.chempr.2017.10.005

3. Tien NT, Jeon S, Kim DI, et al. A flexible bimodal sensor array for simultaneous sensing of pressure and temperature. *Adv Mater*. 2014;26(5):796. doi:10.1002/adma.201302869

4. Wang T, Guo Y, Wan P, Zhang H, Chen X, Sun X. Flexible transparent electronic gas sensors. *Small*. 2016;12(28):3748. doi:10.1002/smll.201601049

5. Salvatore GA, Munzenrieder N, Kinkeldei T, et al. Wafer-scale design of lightweight and transparent electronics that wraps around hairs. *Nat Commun*. 2014;5(1):2982. doi:10.1038/ncomms3982

6. Wang S, Xu J, Wang W, et al. Skin electronics from scalable fabrication of an intrinsically stretchable transistor array. *Nature*. 2018;555 (7694):83. doi:10.1038/nature25494

7. Minev IR, Pavel M, Arthur H, et al. Electronic dura mater for long-term multimodal neural interfaces. *Science*. 2015;347 (6218):159. doi:10.1126/science.1260318

8. Khodagholy D, Doublet T, Quilichini P, et al. In vivo recordings of brain activity using organic transistors. *Nat Commun*. 2013;4 (1):1575. doi:10.1038/ncomms2573

9. Benjamin C-K T, Alex C, Andre B, et al. A skin-inspired organic digital mechanoreceptor. *Science*. 2015;350(6258):313. doi:10.1126/science.aaa9306

10. Kim DH, Lu N, Ma R, et al. Epidermal electronics. *Science*. 2011;333(6044):838. doi:10.1126/science.1206157

11. Boutry CM, Kaizawa Y, Schroeder BC, et al. A stretchable and biodegradable strain and pressure sensor for orthopaedic application. *Nat Electron*. 2018;1(5):314. doi:10.1038/s41928-018-0071-7

12. Zang Y, Shen H, Huang D, Di CA, Zhu D. Semiconducting nanowire-based optoelectronic fibers. *Adv Mater*. 2017;29(27). doi:10.1002/adma.201700681

13. Hong SY, Lee YH, Park H, et al. Stretchable active matrix temperature sensor array of polyaniline nanofibers for electronic skin. *Adv Mater*. 2016;28(5):930. doi:10.1002/adma.201504659

14. Ren X, Pei K, Peng B, et al. A low-operating-power and flexible active-matrix organic-transistor temperature-sensor array. *Adv Mater*. 2016;28(24):4832. doi:10.1002/adma.201600040

15. Zhu C, Chortos A, Wang Y, et al. Stretchable temperature-sensing circuits with strain suppression based on carbon nanotube transistors. *Nat Electron*. 2018;1(3):183. doi:10.1038/s41928-018-0041-0

16. Zhao D, Fabiano S, Berggren M, Crispin X. Ionic thermoelectric gating organic transistors. *Nat Commun*. 2017;8(1):14214. doi:10.1038/ncomms14214

17. Jung MC, Leyden MR, Nikiforov GO, et al. Flat-lying semiconductor–insulator interfacial layer in DNTT thin films. *ACS Appl Mater Interfaces*. 2015;7(3):1833. doi:10.1021/am507528e

18. Hayashi R, Sato A, Ofuji M. et al., 42.1: Invited paper: improved amorphous In-Ga-Zn-O TFTs, Presented at Sid Symposium Digest of Technical Papers; 2008.

19. Kenji N, Hiromichi O, Akihiro T, Toshio K, Masahiro H, Hideo HJN. Room-temperature fabrication of transparent flexible thin-film transistors using amorphous oxide semiconductors. *Nature*. 2004;432 (7016):488. doi:10.1038/nature03090

20. Jin SH, Kang SK, Cho IT, et al. Water-soluble thin film transistors and circuits based on amorphous indium–gallium–zinc oxide. *ACS Appl Mater Interfaces*. 2015;7(15):8268. doi:10.1021/acsami.5b00086

21. Gavryushin V, Račiukaitis G, Juodžbalis D, Kazlauskas A, Kubertavičius VJJOCG. Characterization of intrinsic and impurity deep levels in ZnSe and ZnO crystals by nonlinear spectroscopy. *J Cryst Growth*. 1994;138(1–4):924. doi:10.1016/0022-0248(94)90933-4

22. Takechi K, Nakata M, Eguchi T, Yamaguchi H, Kaneko S. *Jpn J Appl Phys*. 2009;48.

23. Godo H, Kawae D, Yoshitomi S, et al. Temperature dependence of transistor characteristics and electronic structure for amorphous In–Ga–Zn-Oxide thin film transistor. *Jpn J Appl Phys*. 2010;49 (3):03CB04. doi:10.1143/JJAP.49.03CB04

24. Ji KH, Kim J-I, Mo Y-G, et al. Comparative study on light-induced bias stress instability of IGZO transistors With SiN$_x$ and SiO$_2$ gate dielectrics. *IEEE Electr Device L*. 2010;31(12):1404. doi:10.1109/LED.2010.2073439

25. Ji KH, Kim J-I, Jung HY, et al. *Appl Phys Lett*. 2011;98.

26. Hossain Chowdhury MD, Migliorato P, Jang J. Temperature dependence of negative bias under illumination stress and recovery in amorphous indium gallium zinc oxide thin film transistors. *Appl Phys Lett*. 2013;102(14):143506. doi:10.1063/1.4801762

27. Niang KM, Barquinha PMC, Martins RFP, Cobb B, Powell MJ, Flewitt AJ. A thermalization energy analysis of the threshold voltage shift in amorphous indium gallium zinc oxide thin film transistors under positive gate bias stress. *Appl Phys Lett*. 2016;108(9):093505. doi:10.1063/1.4943249

28. Lee J-M, Cho I-T, Lee J-H, Kwon H-I. *Appl Phys Lett*. 2008;93.

29. Lopes ME, Gomes HL, Medeiros MCR, Barquinha P, Ferreira IJAPL. Gate-bias stress in amorphous oxide semiconductors thin-film transistors. *Appl Phys Lett*. 2009;95(6):H161. doi:10.1063/1.3187532

30. Chen T-C, Chang T-C, Hsieh T-Y, et al. *Appl Phys Lett*. 2011;99.